



# OPEN NELL2 suppresses epithelial-mesenchymal transition and induces ferroptosis via notch signaling pathway in HCC

Shiqi Liu<sup>1,2,3</sup>, Haomin Wu<sup>1,2,3</sup>, Pengjie Zhang<sup>1</sup>, Haonan Zhou<sup>1</sup>, Di Wu<sup>1</sup>, Yifan Jin<sup>1,2</sup>, Hongwei Yang<sup>1,2</sup>, Ruilin Xing<sup>1</sup>, Yubo Wu<sup>1</sup> & Gang Wu<sup>1,2</sup>✉

Although various malignant tumors have been associated with the aberrant expression of Neural Epidermal Growth Factor-Like 2 (NELL2), its involvement in hepatocellular carcinoma (HCC) has not been previously documented. In this study, NELL2, recognized as a crucial tumor-suppressor gene, was found to be infrequently expressed in HCC. In vitro experiments demonstrated that the overexpression of NELL2 significantly inhibited the proliferation, migration, and invasion of liver cancer cells, whereas the suppression of NELL2 markedly enhanced these oncogenic properties. Further investigation revealed that NELL2 impedes epithelial-mesenchymal transition (EMT) via the Notch signaling pathway. Inhibition of the Notch pathway reversed the increased tumor proliferation, migration, and invasion observed following the downregulation of NELL2 expression. Notably, gene enrichment analysis and in vitro studies indicated that NELL2 effectively induced ferroptosis in HCC cells, as evidenced by increased levels of cellular malondialdehyde (MDA), iron, and Reactive Oxygen Species (ROS), alongside decreased glutathione (GSH) levels. The blockade of the Notch signaling pathway substantially diminished NELL2's capacity to induce ferroptosis. In summary, our findings suggest that NELL2 modulates the Notch signaling pathway to inhibit EMT and promote ferroptosis. Consequently, NELL2 may serve as a novel therapeutic target, potentially functioning as a tumor suppressor gene in HCC.

**Keywords** HCC, NELL2, Notch pathway, EMT, Ferroptosis

HCC, the most common type of liver cancer, results in the deaths of millions globally annually due to its high rates of occurrence and fatality<sup>1,2</sup>. The most recent Global Cancer Statistics Report shows that HCC is the sixth most frequently diagnosed cancer and the third highest cause of cancer-related mortality<sup>3</sup>. The disease's high death rate is partially attributed to its lack of symptoms in the initial phase<sup>4,5</sup>. Due to its high malignancy, the outlook for HCC is grim, with a median survival of just 11 months and a 5-year survival rate of only 18%<sup>6</sup>. Improving patient outcomes relies heavily on the advancement of individualized therapy approaches and a comprehensive comprehension of the progression mechanism of HCC<sup>7,8</sup>.

NELL2, a glycoprotein that is secreted, contains multiple VWC domains and EGF-like domains, resembling neural epidermal growth factor-like 2<sup>9,10</sup>. Research has indicated a connection between NELL2 expression and the development and specialization of nerve cells<sup>11</sup>. In addition, there is relatively little research on NELL2 in cancer, and a few reports indicate that NELL2 expression and function have also been found to be altered in tumors of the nervous system<sup>12</sup>, bladder cancer<sup>13</sup>, and lung cancer<sup>14</sup>. The protein encoded by the NELL2 gene functions as a component of the extracellular matrix, facilitating cell-to-cell and cell-to-extracellular matrix adhesion, thereby influencing cell migration and localization<sup>15</sup>. Furthermore, NELL2 is implicated in angiogenesis, potentially through the regulation of endothelial cell proliferation, migration, and lumen formation, contributing to the development of new blood vessels<sup>16</sup>. However, the function and molecular mechanism of NELL2 in HCC remain unknown.

<sup>1</sup>Hepatobiliary Surgery Department, First Hospital of China Medical University, No.155, Nanjingbei Street, Shenyang 110001, Liaoning, People's Republic of China. <sup>2</sup>Key Laboratory of General Surgery of Liaoning Province, First Hospital of China Medical University, No.155, Nanjingbei Street, Shenyang 110001, Liaoning Province, People's Republic of China. <sup>3</sup>Shiqi Liu and Haomin Wu contributed equally to this work. ✉email: cmuwgzwl@126.com

The Notch signaling pathway is a well-established and essential mechanism that regulates critical decisions concerning cell fate in mammals, including the maintenance of stem cells, cell differentiation, and the promotion of cell proliferation. Disruption of the Notch pathway is intricately linked to tumorigenesis<sup>17–20</sup>. Dysfunction in the Notch pathway can impact the development, advancement, spread, and spread of various cancer types, such as liver cancer<sup>21</sup>, bladder cancer<sup>22</sup>, and prostate cancer<sup>23</sup>. The Notch signaling pathway is composed of the Notch receptor (Notch1–4), Notch ligand, DNA-binding protein, and Notch regulatory molecules<sup>24</sup>. Notch1, a member of the Notch receptor family, functions as a transmembrane signal transducer that plays a role in maintaining tissue balance<sup>25</sup>. Research has demonstrated that Notch1 functions as both an oncogene and a tumor suppressor in various tumor types<sup>26</sup>. In the case of head and neck squamous cell carcinoma (HNSCC), there is a heightened activation of Notch1/Hes1 signaling<sup>27</sup>. Conversely, Notch1 functions as a tumor suppressor in neuroendocrine tumors<sup>28,29</sup>. However, there have been no documented studies examining the regulatory interaction between NELL2 and the Notch signaling pathway. In our research, we demonstrated that the overexpression of NELL2 inhibited liver cancer cell proliferation, migration, invasion, and EMT via the Notch signaling pathway. Furthermore, existing literature indicates that the Notch pathway serves as a pivotal upstream regulator of EMT<sup>19</sup>.

Ferroptosis is a type of cell death that relies on iron and lipid peroxidation, characterized by elevated iron levels, a dysfunctional lipid repair mechanism, and lipid peroxidation, leading to the destruction of cell membranes and ultimately cell death<sup>30,31</sup>. Multiple cancers are closely associated with dysregulation of ferroptosis<sup>32</sup>. Our findings also revealed a positive correlation between NELL2 expression and ferroptosis, with *in vitro* experiments confirming that NELL2 overexpression significantly induces ferroptosis in tumor cells. Recent studies have identified Notch1 and Notch3, components of the Notch signaling pathway, as inhibitors of ferroptosis in non-small cell lung cancer (NSCLC)<sup>33</sup>. This observation led us to hypothesize that NELL2 might facilitate ferroptosis through the Notch signaling pathway. Subsequent experiments conducted in our study validated the hypothesis.

In conclusion, this study demonstrates that NELL2 expression is downregulated in HCC and is significantly correlated with poor prognosis. Furthermore, NELL2 markedly inhibits tumor progression and EMT via the Notch signaling pathway. Additionally, NELL2 facilitates ferroptosis in liver cancer cells through the same pathway. These findings elucidate a novel mechanism by which NELL2 exerts its anticancer effects against HCC.

## Materials and methods

### Patient tissue samples

HCC tissue samples were obtained from 71 patients diagnosed with the condition, all of whom underwent standard hepatic surgery at the First Affiliated Hospital of China Medical University between January 2018 and January 2019. Patient survival was monitored over a five-year period. 71 pairs of tumor tissues and their corresponding non-cancerous parenchyma were promptly cryopreserved in liquid nitrogen and subsequently stored at  $-80^{\circ}\text{C}$  following excision. The study protocol received approval from the Institutional Ethics Committee of China Medical University (AF-SOP-07-1.1-01). Informed consent was given by all patients.

### Cell culture

Liver cancer cell lines Huh-7, Bel-7402, SK-Hep-1, HepG-2, and HCC-LM3, along with the normal liver cell line LO2, were acquired from the Shanghai Cell Bank in Shanghai, China. Cell lines were grown in high-glucose DMEM and RPMI-1640 medium with 10% FBS and 1% penicillin/streptomycin at  $37^{\circ}\text{C}$  in a 5%  $\text{CO}_2$  humidified environment. MK0752, an inhibitor of the Notch signaling pathway, was dissolved in dimethyl sulfoxide and incubated for 48 h to achieve a final concentration of 5 nM in the culture medium.

### Knockdown and overexpression of NELL2

All cells were transfected with lentivirus, including knockout vector (sh-NELL2), knockout control vector (sh-NC), overexpression vector (NELL2), and overexpression control vector (Ctrl) purchased from Gene-chem. The procedure for virus transfection using a 12-well plate is as follows: Prepare a cell suspension with a density of  $3\text{--}5 \times 10^4$  cells/ml using a complete culture medium. Dispense 1 ml of the cell suspension into each well and incubate at  $37^{\circ}\text{C}$  for 16–24 h until cell confluence reaches 20–30%. Typically, the cell count after 24 h of culture is approximately double the initial plating density. Subsequently, transfect the cells with lentivirus, determining the amount of virus based on the multiplicity of infection (MOI), calculated as  $\text{MOI} = (\text{virus titer} \times \text{virus volume}) / \text{number of cells}$  (Huh-7: MOI = 5, Bel-7402: MOI = 20, HepG-2: MOI = 10, HCC-LM3: MOI = 10). Additionally, employ the transfection-enhancing reagent Ha, diluted from a  $25 \times$  stock solution to  $1 \times$  working concentration. Following transfection, perform cell selection using puromycin at a concentration of  $2 \mu\text{g/ml}$ . Cells that have undergone selection for two weeks are suitable for subsequent functional assays, the interference sequences of NELL2 was list in Supplementary Table S1.

### Immunohistochemical (IHC) staining analysis

Wax blocks were constructed from a total of 30 HCC and paired with adjacent nontumor tissue samples. We randomly select 10 samples from each group according to the high, medium, and low differentiation degrees of the postoperative pathological results of all the 71 samples, with a total of 30 samples. The specimen wax blocks were then placed on a slicer and cut into  $4 \mu\text{m}$  sections. Afterward, the sections were treated to remove wax, and the process of repairing antigens was finished. After 15 min of serum blocking, the primary and secondary antibodies (NELL2, Abcam, 1:100; HRP Goat Anti Rabbit IgG, Immunoway, 1:500) were incubated, and finally, 3,3'-diaminobenzidine staining was performed. Hematoxylin staining was also done. The dried glass slide was placed in a panoramic scanning imaging system for full-film scanning.

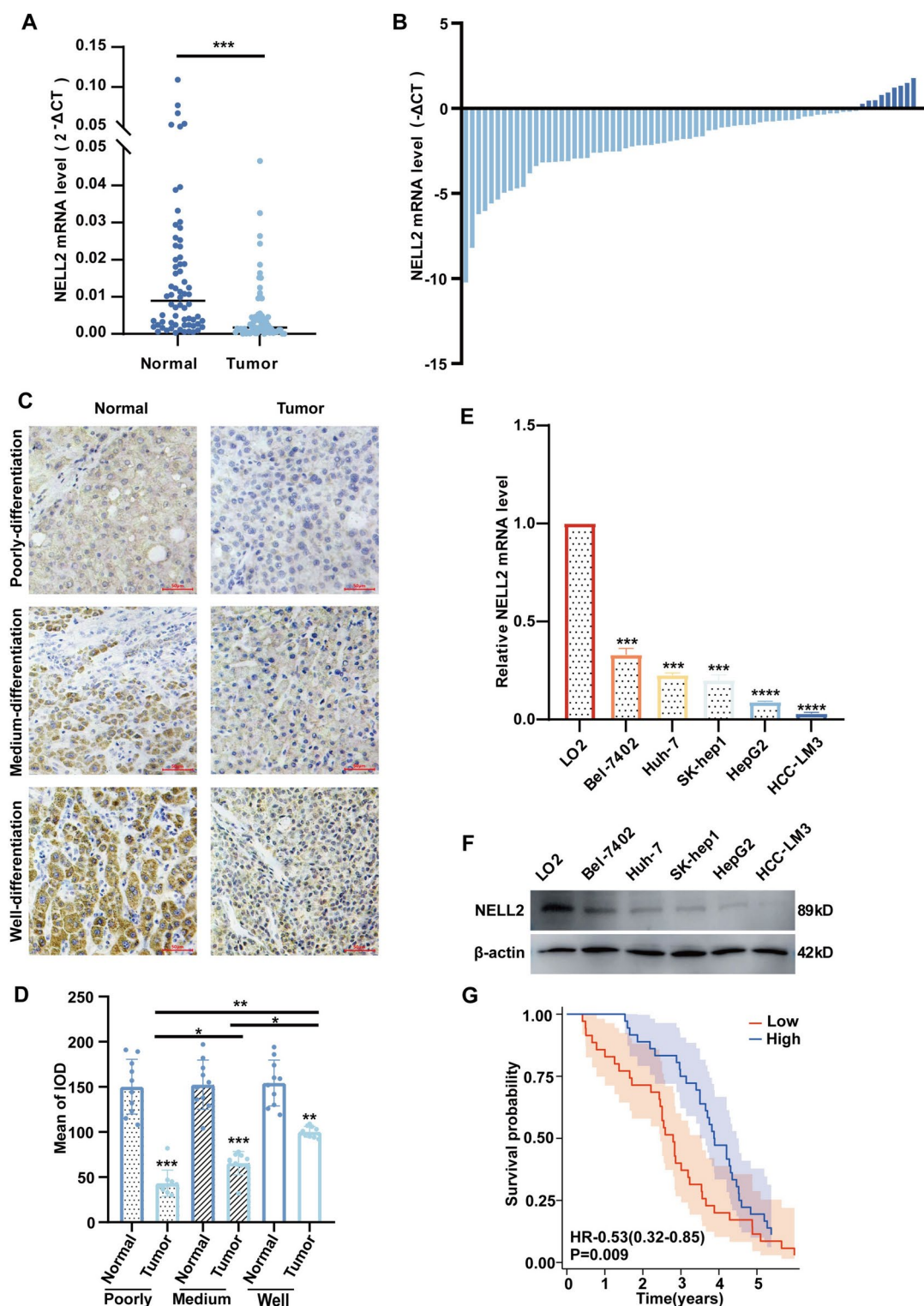


**Fig. 1.** (A) Relative mRNA expression level ( $2^{-\Delta CT}$ ) of NELL2 in HCC patients (n=71); (B) Relative mRNA expression level ( $-\Delta CT$ ) of NELL2 from matched Normal liver tissues and HCC tissues in HCC patients (n=71); (C,D) Immunohistochemical (IHC) images of NELL2 in the HCC tissues and normal liver tissues (50 $\times$ , 200 $\times$ ); (E) Relative mRNA expression level of NELL2 in HCC cell lines. LO2 was used as control; (F) Relative protein expression level of NELL2 in HCC cell lines. LO2 was used as control; (G) Survival analysis (Kaplan-Meier) of NELL2 from 71 HCC patients in 5 years.

Parameters	Total	NELL2 expression		P value
		Low	High	
Gender				0.409
Female	27	12	15	
Male	44	24	20	
Age (years)				0.350
≤ 50	15	6	9	
> 50	56	30	26	
Encapsulation				0.712
Yes	32	17	15	
No	39	19	20	
Tumor size (cm)				<b>0.029</b>
≤ 3	20	6	14	
> 3	51	30	21	
Tumor number				0.531
Single	42	20	22	
Multiple	29	16	13	
MVI				<b>0.006</b>
M0	35	12	23	
M1 + M2	36	24	12	
Cirrhosis				0.188
Negative	27	11	16	
Positive	44	25	19	
Thrombosis				0.327
Yes	51	24	27	
No	20	12	8	
Ascites				0.368
Yes	54	29	25	
No	17	7	10	
HBsAg				0.737
Negative	23	11	12	
Positive	48	25	23	
AFP(ng/ml)				0.417
≤ 400	56	27	29	
> 400	15	9	6	
PLT(10 <sup>9</sup> /L)				0.547
≤ 100	20	9	11	
> 100	51	27	24	
ALT (U)				0.511
≤ 40	46	22	24	
> 40	25	14	11	
Albumin (g/L)				0.411
≤ 40	29	13	16	
> 40	42	23	19	
Bilirubin (umol/L)				0.120
≤ 17.1	43	25	18	
> 17.1	28	11	17	
TNM stage				0.268
I	29	17	12	
II + III + IV	42	19	23	
Recurrence				0.556
Continued				

Parameters	Total	NELL2 expression		P value
		Low	High	
Yes	37	20	17	
No	34	16	18	
Survival				<b>0.046</b>
Died	10	8	2	
Alive	61	28	33	

**Table 1.** The correlation between NELL2 expression levels and clinicopathological factors in HCC patients. Bold indicates statistical significance,  $P < 0.05$ .

### Quantitative real-time PCR (qRT-PCR)

Total RNA was isolated from HCC tissues and cells using the TRIZOL reagent (Invitrogen), the quantified concentration of the extracted RNA is 2 µg/µl. And then converted to complementary DNA (cDNA) with the PrimeScript RT reagent kit using gDNA Eraser (RR047A, Takara) as per kit directions. TB Green® was employed to identify the gene transcript level via the Light Cycler 480 II Real-Time PCR system (Roche Diagnostics). The primer sequence of NELL2 and GAPDH is listed in Supplementary Table S2. The primers were designed and synthesized by Sangon Biotech. The cycle threshold (Ct) was determined according to the total number of cycles required for the TB Green® signal to cross the threshold. The fold-change in transcript levels was computed using the  $2^{-\Delta\Delta C_t}$  formula.

### Western blotting

Proteins from HCC cells were isolated using a lysis buffer containing protease, phosphatase, and PMSE. After quantifying the protein to 2 µg/µl, the sample size for each pore in the experiment was 10 µl. Then separated with SDS-PAGE and transferred to PVDF membranes based on their molecular size. Afterwards, the PVDF filters were obstructed with a mixture of Tris-buffered saline and 0.1% Tween 20 (TBST) combined with 5% skim milk, then exposed to primary antibodies for an overnight incubation at 4 °C. Following three washes with TBST, each lasting 15 min, the membranes were incubated with the corresponding secondary antibodies for 1.5 h. The signal was detected using chemiluminescence (Amersham Image Quant 800). The antibodies and their dilutions are listed in Supplementary Table S3. β-actin was served as the internal control. The original images of all gels are cited in Supplementary Material 1.

### Cell counting kit-8 (CCK8) and colony formation assays

For the CCK8 assay, transfected cancer cells were seeded into a 96-well plate, with 3000 cells per well. Five replicate wells were set, and CCK8 was added 1 h before detection from day 0 to day 4 using the Spectra-Max Absorbance Reader (Molecular Devices). For colony formation assays, after transfection, 1000 cells per well were inoculated into a six-well plate for clone formation assay, and three repeated wells were set up. Two weeks later, the colony was stained with crystal violet after methanol fixation.

### EdU assay

EdU is a thymidine nucleoside analog that can replace thymine to participate in synthesized DNA molecules during DNA replication. EdU-specific reactions can directly and accurately detect DNA replication activity and are widely used in studies such as cell proliferation and differentiation. Cancer cells were seeded 24 h in advance in 12-well climbing plates at approximately 30%–40% confluency. Cells were cultured in a medium with EdU for 2 h and then analyzed with the BeyoClick™EdU kit (C0071S) following the provided guidelines. Subsequently, an appropriate amount of 1 × DAPI reaction solution was used for DNA staining. Images were captured using a multichannel fluorescence microscope (Leica DMI8, THUNDER Imager, Germany).

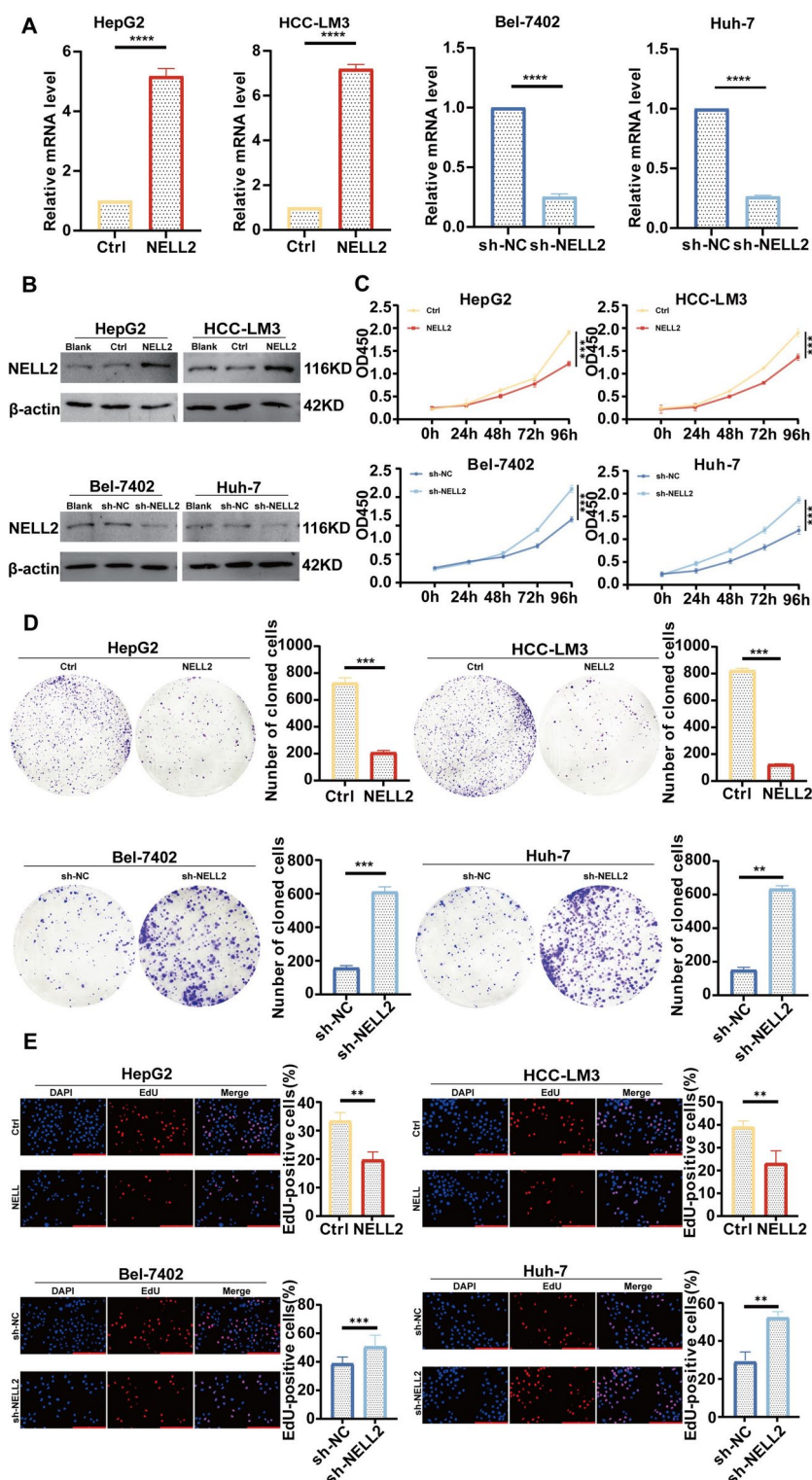
### Transwell and Wound healing assays

In the migration test, 20,000 cancer cells were placed in the top chamber with 200 µL of RPMI-1640 medium or high-glucose DMEM (lacking FBS), while the lower chamber had 600 µL of the culture medium with 20% FBS. Prior to the experiment, 50 µL of Matrigel (BD Bioscience, USA) was added to the Transwell chamber (Costar, USA) for the invasion assay with a 6-h incubation period. Following a 48-h incubation period at 37 degrees Celsius in the presence of 5% carbon dioxide, the cells within the compartment were eliminated using a cotton swab. After staining the cells on the basement membrane of the chamber with hematoxylin and eosin and fixing them with neutral resin, they were imaged using a Leica DM3000 microscope from Leica in Wetzlar, Germany. Cell counting was performed using the Image-Pro6.0 software. For the wound healing assay,  $5 \times 10^4$  transfected cells were plated in six-well plates and cultured overnight. A 200 µL pipettor was used to nick the single-cell layer. Areas of the wound were viewed at 200× magnification under an inverted light microscope (Leica DMI3000B). Pictures were taken at 0 h and 24 h following the creation of the scratch.

### Ferroptosis analyses and detection

RNA-sequencing expression (level 3) profiles and corresponding clinical information for LIHC were downloaded from the TCGA dataset (<https://portal.gdc.com>). The GSVA package in R software was utilized for analysis, with the parameter set as method = 'ssgsea'. Spearman correlation was used to analyze the relationship between genes





and pathway scores. R version 4.0.3 was used to implement various analysis techniques and R packages.  $p < 0.05$  was deemed to be statistically significant. ROS, MDA, GSH, and iron levels were assessed with specific assay kits as per the instructions provided.

### Statistical analyses

All experiments were independently repeated three times. Values were presented as the average plus standard deviation. Statistical significance was assessed by conducting a two-tailed student's t-test or one-way ANOVA. Correlations between the measured variables were analyzed using the Spearman rank correlation test. Kaplan–Meier curves were employed to estimate survival probabilities. SPSS software (25.0) was used for statistical analysis. A P-value less than 0.05 indicated statistical significance.

◀ **Fig. 2.** (A) The mRNA expression level of NELL2 in HCC cell lines after transfection with NELL2 knockdown (Bel-7402, Huh-7) or overexpression (HepG2, HCC-LM3) lentiviruses detected by qRT-PCR, HCC cell lines transfected by negative control lentiviruses was used as control; (B) The protein expression levels of NELL2 in HCC cell lines after transfection with knockdown (Bel-7402, Huh-7) or overexpression (HepG2, HCC-LM3) lentiviruses detected by Western Blot, HCC cell lines transfected by negative control lentiviruses was used as control; (C) Cell proliferation detected by CCK-8 in HCC cell lines after transfection with NELL2 knockdown (Bel-7402, Huh-7) or overexpression (HepG2, HCC-LM3) lentiviruses, HCC cell lines transfected by negative control lentiviruses was used as control; (D) Cell proliferation detected by colony formation assays in HCC cell lines after transfection with NELL2 knockdown (Bel-7402, Huh-7) or overexpression (HepG2, HCC-LM3) lentiviruses, HCC cell lines transfected by negative control lentiviruses was used as control; (E) Cell proliferation detected by EDU in HCC cell lines after transfection with NELL2 knockdown (Bel-7402, Huh-7) or overexpression (HepG2, HCC-LM3) lentiviruses, HCC cell lines transfected by negative control lentiviruses was used as control.

## Results

### NELL2 expression is low and suggests poor prognosis in HCC patients

To investigate the expression of NELL2 in HCC tissues, HCC tissues from 71 patients and paired adjacent tissues were selected. The mRNA level of NELL2 was detected using qRT-PCR. The findings indicated a notable decrease in the mRNA expression of NELL2 in HCC tissues compared to neighboring noncancerous tissues (Fig. 1A). Further analysis revealed that the remaining 62 patients demonstrated low expression, and only nine patients exhibited a high expression of NELL2 in the liver cancer tissue (Fig. 1B). IHC staining signified that NELL2 was predominantly distributed in the cytoplasm, and its expression level in different differentiation HCC tissues was significantly lower than that in paired para-cancerous tissues (Fig. 1C,D). To select cell lines for subsequent experiments, the human normal liver immortalized cell line LO2 was chosen as the normal control. qRT-PCR and WB were utilized to measure the mRNA and protein levels in five liver cancer cell lines. The results suggested that the NELL2 expression levels in hepatoma cell lines were notably decreased compared to LO2 (Fig. 1E,F). The correlation between NELL2 expression levels and clinicopathological factors in HCC patients was assessed using qRT-PCR results. The findings showed that the tumor size was greater in the low-expression group compared to the high-expression group ( $P = 0.029$ ). Moreover, the low-expression group was more prone to microvascular invasion (MVI,  $P = 0.006$ ) and exhibited a worse survival prognosis ( $P = 0.046$ ). Nevertheless, there were no notable variations in additional pathological information among the two categories (Table 1). Kaplan–Meier was utilized to examine the correlation between NELL2 expression in HCC tissues and prognosis. The findings indicated that a decreased level of NELL2 in HCC tissues was associated with an unfavorable outlook (Fig. 1G).

### NELL2 inhibits proliferation of HCC

In Bel-7402 and Huh-7 cell lines, NELL2-knockdown stable transfection cell lines (sh-NC and sh-NELL2) constructed using the NELL2-knockdown virus vector. In HepG2 and HCC-LM3 cell lines, NELL2-overexpression stable transfection cell lines (Ctrl and NELL2) were constructed using the NELL2 overexpression lentiviral vector. The transfection efficiency of NELL2 in cancer cells was detected using qRT-PCR and WB. The findings indicated a notable decrease in the expression of NELL2 at both mRNA and protein levels in knockdown cells, while there was a significant increase in overexpression cells (Fig. 2A,B). CCK-8 assay suggested that after NELL2 knockdown, the cell proliferation rate increased significantly within 96 h. On the contrary, the cell proliferation rate decreased significantly after NELL2 overexpression (Fig. 2C). Colony formation assays indicated that the number of cell colonies increased significantly after NELL2 knockdown, whereas it decreased significantly after NELL2 overexpression (Fig. 2D). The EdU experiment also yielded similar results; the proportion of proliferating cells increased significantly after NELL2 knockdown but decreased significantly after its overexpression (Fig. 2E).

### NELL2 inhibits migration and invasion of HCC

Cell migration was assessed using the scratch and transwell assays to investigate the impact of NELL2. After 24 h, cells with reduced NELL2 levels showed a notably faster healing rate compared to the control group. Cells with increased NELL2 expression exhibited a notably reduced 24-h wound healing rate compared to the control group (Fig. 3A,B). Knockdown of NELL2 significantly enhanced cell migration and invasion based on transwell assay. However, after the overexpression of NELL2, the migration and invasion abilities of the cells decreased significantly (Fig. 3C,D). In comparison to the control group, silencing NELL2 led to a reduction in level of E-cadherin expression and elevation in the levels of N-cadherin, Snail1, and  $\beta$ -catenin expression. Conversely, upregulation of NELL2 led to a rise in E-cadherin levels and a drop in N-cadherin, Snail1, and  $\beta$ -catenin expression. The findings indicate that NELL2 could impact the metastatic potential of liver cancer cells by influencing EMT (Fig. 3E).

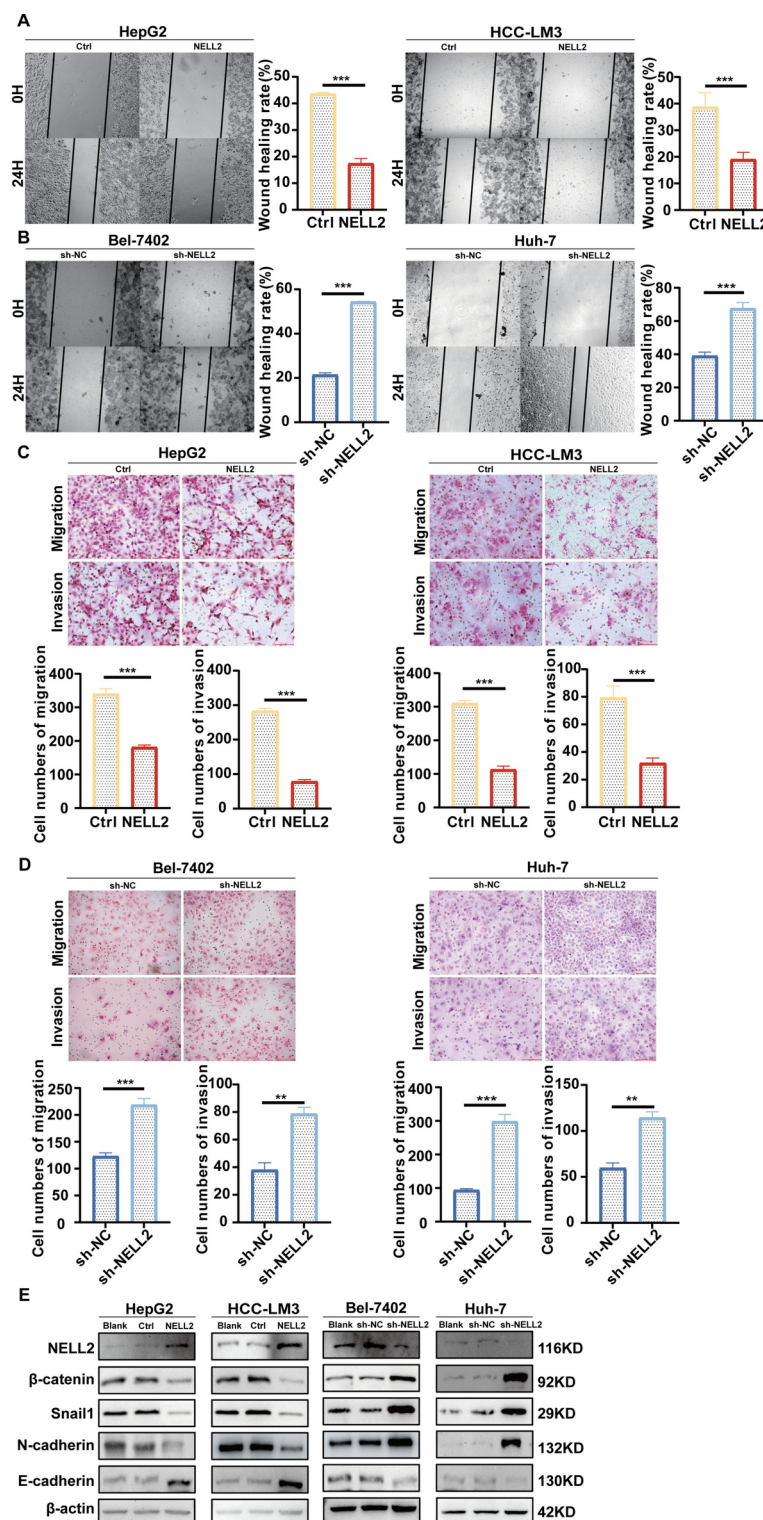


**Fig. 3.** (A,B) Transwell migration/invasion assay in HCC cell lines after transfection with NELL2 knockdown (Bel-7402, Huh-7) or overexpression (HepG2, HCC-LM3) lentiviruses, HCC cell lines transfected by negative control lentiviruses was used as control; (C,D) Wound healing assay in HCC cell lines after transfection with NELL2 knockdown (Bel-7402, Huh-7) or overexpression (HepG2, HCC-LM3) lentiviruses, HCC cell lines transfected by negative control lentiviruses was used as control; (E) The protein expression levels of JAG1, Notch1, NICD and Hes1 in HCC cell lines after transfection with knockdown (Bel-7402, Huh-7) or overexpression (HepG2, HCC-LM3) lentiviruses detected by Western Blot, HCC cell lines without transfection was used as blank control, HCC cell lines transfected by negative control lentiviruses was used as negative control.



## NELL2 suppresses the proliferation, migration, invasion and EMT of HCC via the Notch signaling pathway

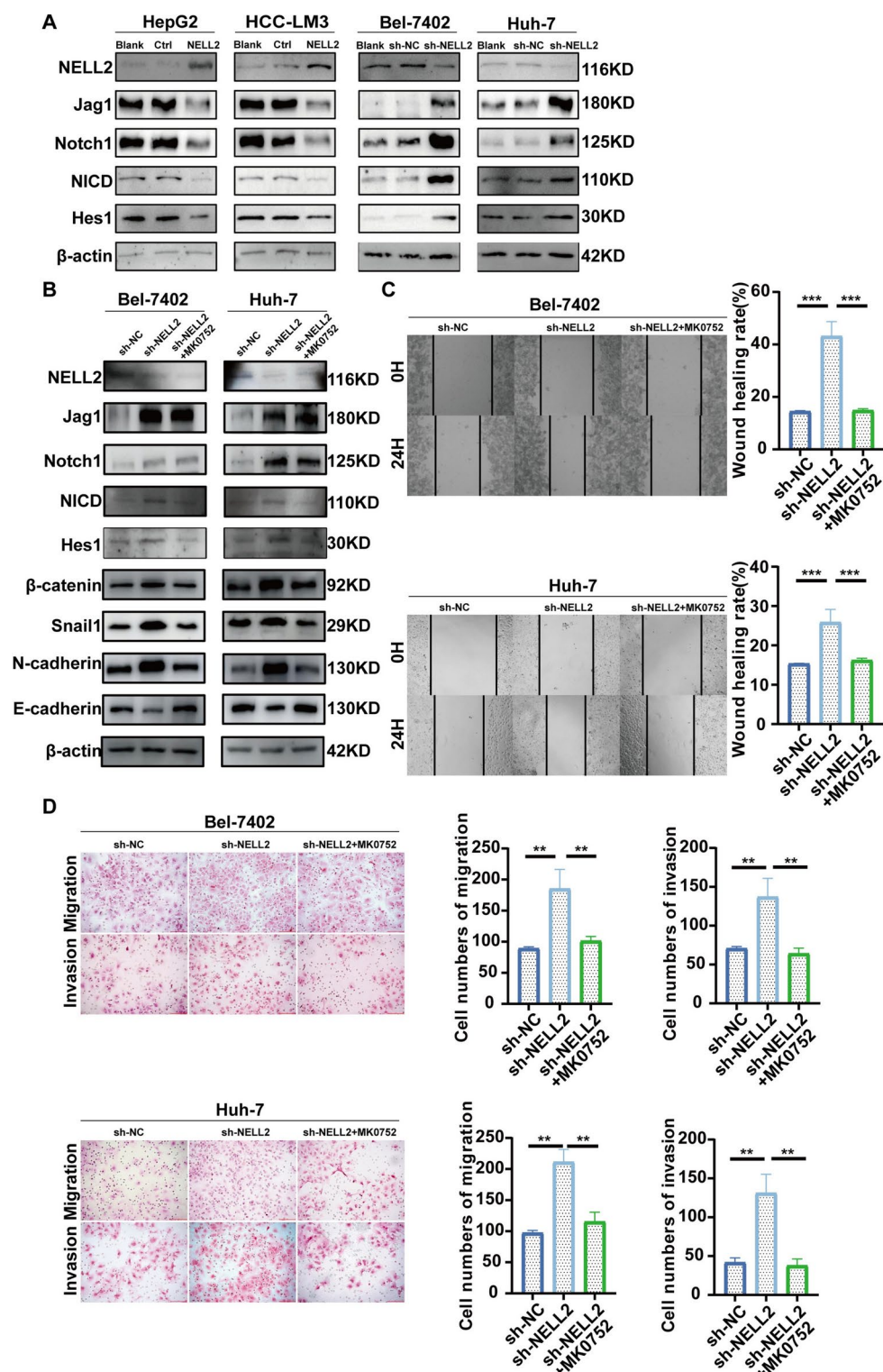
Experimental findings indicate that NELL2 effectively inhibits the Notch signaling pathway. Given the established association between the Notch signaling pathway and cancer cell proliferation and metastasis, we propose that NELL2 impedes the proliferative, migratory, and invasive capabilities of liver cancer cells through this pathway. Western blotting was utilized to measure the levels of expression of key components in the Notch signaling pathway. The findings indicated that when the expression of NELL2 decreased, the expression levels of JAG1 and Notch1 increased significantly. The expression levels of NICD and the downstream index Hes1 also increased. When NELL2 expression increased, JAG1, Notch1, NICD, and Hes1 expression decreased (Fig. 4A). MK0752, a Notch pathway inhibitor, was utilized to determine its IC<sub>50</sub> in Huh-7 and Bel-7402 cells, both of which were found to be 5 nM (Supplementary Fig. S1A). As a selective inhibitor of NICD production, MK0752 significantly reduced NICD expression and restored Hes1 expression. These findings suggest that the expression levels of Notch1 and Jag1 were unaffected by MK0752. Notably, the inhibition of NICD and Hes1 also altered EMT-related phenotypes. Upon NICD suppression, the expression levels of EMT-associated proteins ( $\beta$ -catenin, Snail 1, E-cadherin, and N-cadherin) reverted to baseline levels observed in untreated cells (Fig. 4B). The results allude to the EMT status of tumor cells being regulated by the Notch pathway. The Notch pathway inhibitor MK0752 was introduced to inhibit the activation of the Notch pathway in NELL2-knockdown cells to investigate its potential impact on cell proliferation, migration, and invasion. The addition of MK0752 restored the increased migration and invasion ability caused by NELL2 downregulation according to the wound healing (Fig. 4C) and transwell assays (Fig. 4D). In addition, the addition of MK0752 also restored the increased proliferation ability caused by NELL2 downregulation (Supplementary Fig. S1B–E).

## NELL2 induces ferroptosis via the Notch pathway

According to previous results, NELL2 regulates the Notch signaling pathway. We also performed pathway correlation enrichment analysis on NELL2 from the TCGA database, and found that NELL2 is closely related to ferroptosis (Fig. 5A). In previous research, Notch1 and Notch3 have been reported as potential negative regulators of liver cancer ferroptosis<sup>34</sup>. Thus, we proposed that NELL2 may regulate ferroptosis via the Notch pathway. RSL3, functioning as an inhibitor of glutathione peroxidase, impedes the transport of cysteine and glutamate amino acids, thereby inhibiting glutathione synthesis and serving as an inducer of ferroptosis. The levels of MDA, ROS, and GSH were also evaluated, given their critical roles in the ferroptosis process. The results demonstrated a reduction in MDA levels in cells following the suppression of NELL2 expression, with a more significant decrease observed upon RSL3 administration. Conversely, up-regulation of NELL2 resulted in a marked increase in MDA content within the cells, with this effect being further amplified after RSL3 treatment. Administration of MK0752 subsequently rescued the decrease in MDA production caused by NELL2 knockdown (Fig. 5B). The ROS levels exhibited a pattern consistent with the fluctuations observed in MDA levels (Fig. 5C), with these differences becoming more pronounced following RSL3 treatment and increasing further after MK0752 administration (Fig. 5D). Notably, intracellular iron overload is a critical marker of ferroptosis. We quantified intracellular iron concentrations utilizing an iron assay kit specific for Fe<sup>2+</sup>. The results demonstrated a decrease in Fe<sup>2+</sup> levels within cells upon the suppression of NELL2 expression, with this reduction becoming more pronounced after RSL3 treatment. Conversely, upregulation of NELL2 resulted in a significant increase in intracellular Fe<sup>2+</sup> levels, again with a more pronounced disparity following RSL3 administration. Administration of MK0752 subsequently led to a reduction in Fe<sup>2+</sup> levels (Fig. 5E). These findings substantiate the role of NELL2 in inhibiting ferroptosis.

## Discussion

Initially discovered to be abundant in the nervous system, NELL2 was recognized for its involvement in neural development<sup>35</sup>. Abnormal NELL2 expression has been linked to several cancerous growths in studies<sup>36–38</sup>. In studies utilizing gene chips and sequencing technology, NELL2 was observed to be a potential pathogenic site for ovarian cancer<sup>39</sup>. In a gene analysis of prostate cancer, normal prostate tissues, and benign prostatic hyperplasia tissues, NELL2 was found to be significantly overexpressed in benign prostatic lesions<sup>40</sup>. A study has reported the presence of a significant difference in the expression of NELL2 between normal bladder tissues and bladder cancer tissues, which may be used as a diagnostic marker for bladder cancer<sup>13</sup>. In renal cell carcinoma, NELL2 has been shown to inhibit the migration of cancer cells, and the hypermethylation of the promoter has been observed to inhibit the effect of NELL2<sup>41</sup>. Researchers have uncovered the differential expression of NELL2 between oral cancer and normal tissues using gene chip sequencing technology. Its low expression level can indicate the poor prognosis of patients, and it may be a potential early diagnostic marker and therapeutic target<sup>42</sup>. In addition, the expression of NELL2 is upregulated during the progression of mucosal leukoplakia to oral squamous cell carcinoma and may be related to the proliferation of cancer cells<sup>38</sup>. The presence of NELL2 in the tumor microenvironment of esophageal squamous cell carcinoma has been confirmed and can affect the prognosis of patients and the sensitivity to immunotherapy<sup>43</sup>. NELL2 predominantly plays a tumor-inhibitory role in gastrointestinal tumors. In colon cancer, mir-22 prevents NELL2 gene inhibition mediated by 1,25 (OH)<sub>2</sub>D<sub>3</sub>, thereby promoting the migration and invasion of tumor cells<sup>37</sup>. In gastric cancer, the tRNA derivative tRF-3017a inhibits the expression of NELL2 and promotes the migration and invasion of cells. The expression level of NELL2 in tumor tissues is significantly correlated with lymph node metastasis ( $P < 0.05$ )<sup>44</sup>. Although NELL2



has been proven to play a major role in various tumors, it has not been reported in HCC. In this study, qRT-PCR, IHC, and WB experiments were used to establish that NELL2 expression was significantly low in HCC and that it was negatively correlated with tumor size, MVI, and survival time of patients. The overexpression of NELL2 was initially confirmed to inhibit the proliferation, migration, and invasion of HCC cells.

Notch signaling pathways are widely considered to be highly conserved cell signaling pathways. Notch receptors, Notch ligands, and intracellular Notch target proteins like Hes1 and Hey1 make up the Notch cascade<sup>45</sup>. It has also been revealed that the Notch signaling pathway is one of the most frequently activated pathways in

◀ **Fig. 4.** (A) The protein expression levels of  $\beta$ -catenin, Snail1, E-cadherin and N-cadherin in HCC cell lines after transfection with knockdown (Bel-7402, Huh-7) or overexpression (HepG2, HCC-LM3) lentiviruses detected by Western Blot, HCC cell lines without transfection were used as blank control, HCC cell lines transfected by negative control lentiviruses was used as negative control; (B) The protein expression levels of JAG1, NOTCH1, NICD and Hes1 in HCC cell lines after transfection with knockdown (Bel-7402, Huh-7) lentiviruses detected by Western blotting, HCC cell lines transfected by negative control lentiviruses and transfected HCC cell lines treated with 5nM DMSO was used as control. Knockdown (Bel-7402, Huh-7) lentiviruses treated with 5nM DMSO or 5nM MK0752, Transfected HCC cell lines treated with 5nM DMSO was used as control; (C) Wound healing assay in HCC cell lines after transfection with NELL2 knockdown (Bel-7402, Huh-7) lentiviruses treated with 5nM DMSO or 5nM MK0752, Transfected HCC cell lines treated with 5nM DMSO was used as control; (D) Transwell migration/invasion assay in HCC cell lines after transfection with NELL2 knockdown (Bel-7402, Huh-7) lentiviruses treated with 5nM DMSO or 5nM MK0752, Transfected HCC cell lines treated with 5nM DMSO was used as control.

tumors, especially in gastrointestinal malignancies, liver cancers, and pancreatic tumors<sup>46–49</sup>. Studies also have shown that the Notch signaling pathway promotes lung cancer<sup>50</sup>. In ovarian cancer cells, the Notch pathway causes growth inhibition and induces apoptosis, suggesting that targeting the Notch pathway may provide new therapeutic approaches<sup>51,52</sup>. A report by Dandawate et al. found that the Notch signaling pathway also regulates colon cancer cell proliferation<sup>53</sup>. Overall, the Notch signaling pathway is essential for cancer development and progression. In our research, we discovered that NELL2 can impede the development and EMT of HCC cells by mean of the Notch signaling pathway. A significant signaling pathway in the regulation of EMT is the Notch pathway, which is activated through the interaction between the Notch receptors and the ligands of neighboring cells<sup>54,55</sup>. In addition, most studies have shown that Notch signaling pathway is involved in EMT. Inhibition of this pathway partially reverts EMT in lung adenocarcinoma cells<sup>56</sup>. ROS can promote EMT and metastasis in HCC through Nrf2/Notch signaling<sup>57</sup>. Earlier studies have suggested that pancreatic cancer cells became gemcitabine resistant after undergoing EMT through the Notch pathway<sup>58</sup>. Since EMT and Notch pathway are tightly correlated, we performed experiments to demonstrate that NELL2 inhibits EMT via Notch signaling.

Our research exhibits a notable limitation due to the absence of theoretical evidence supporting the regulation between NELL2 and the Notch signaling pathway. However, our in vitro experiments demonstrate that NELL2 can modulate the expression of key molecules within the Notch signaling pathway. Regarding the regulation of NELL2, we propose the following explanation: Firstly, the molecular characteristics of NELL2 suggest a potential association with the Notch signaling pathway. NELL2 is a member of the epidermal growth factor (EGF)-like protein family, characterized by multiple EGF-like repeat sequences, which are typically involved in intercellular signaling and receptor binding<sup>59</sup>. Similarly, the Notch receptor contains approximately 36 EGF-like repeat domains, which are essential for ligand recognition and signal activation<sup>60</sup>. Secondly, Notch signaling exhibits a dual function in various cancers, either promoting or inhibiting tumorigenesis, and its aberrant activation is frequently linked to the properties of cancer stem cells<sup>61</sup>. Although research on the role of NELL2 in cancer remains limited, its involvement in cell differentiation and survival suggests that it may influence the expression of downstream target genes, such as HES and MYC, within the Notch pathway by modulating growth factor signaling<sup>62,63</sup>.

In contrast to other forms of cell death, ferroptosis is a newly identified programmed cell death associated primarily with iron metabolism and lipid peroxidation<sup>64</sup>. There is mounting evidence that ferroptosis plays a significant role in tumor progression. Further pathway enrichment analysis of NELL2 based on TCGA revealed a significant correlation with ferroptosis. As a result, we conducted experiments to confirm that NELL2 can indeed induce ferroptosis. It has been demonstrated that Notch1 regulates ferroptosis by altering the expression of GPX4. Furthermore, Notch1 promotes the expression of ankyrin repeats and SOCS box containing 2 (ASB2) through transcriptional modulation, which inhibits ferroptosis, contributing to HCC progression. Therefore, we have reason to speculate whether NELL2 induces ferroptosis by affecting the Notch pathway. When NELL2 is downregulated, iron death inhibition can be rescued with the Notch pathway inhibitor MK0752. But the potential molecular mechanisms still need to be explored.

As a summary, NELL2 has been identified as a critical tumor suppressor gene in HCC (Fig. 6). We also report for the first time the regulatory role that NELL2 plays in Notch signaling. Importantly, NELL2 regulates cancer cells EMT and ferroptosis through the Notch signaling. However, there are still many shortcomings in our research. On the one hand, the potential molecular mechanisms of the NELL2 and Notch pathways are not fully understood, and on the other hand, it is still worth exploring how the Notch pathway regulates ferroptosis in this study.

Based on our experimental results, it suggests the potential of NELL2 as a potential biomarker for liver cancer. Additionally, enhancing the expression level of NELL2 may have a therapeutic effect on clinical liver cancer. Currently, there are various therapeutic methods in clinical practice that exert therapeutic effects by inducing ferroptosis. If NELL2-related therapeutic drugs can be developed and combined with existing treatment methods, it is hoped that the therapeutic effects of these treatment methods can be improved. However, for NELL2 to be applied as a therapeutic target in clinical treatment, more experimental results are needed to verify its safety and effectiveness. Our experiment aims to reveal the possibility of this application. In the future, we will continue to delve deeply into this field, hoping to bring more meaningful experimental results and provide a theoretical basis for the development of clinical drugs for liver cancer treatment.

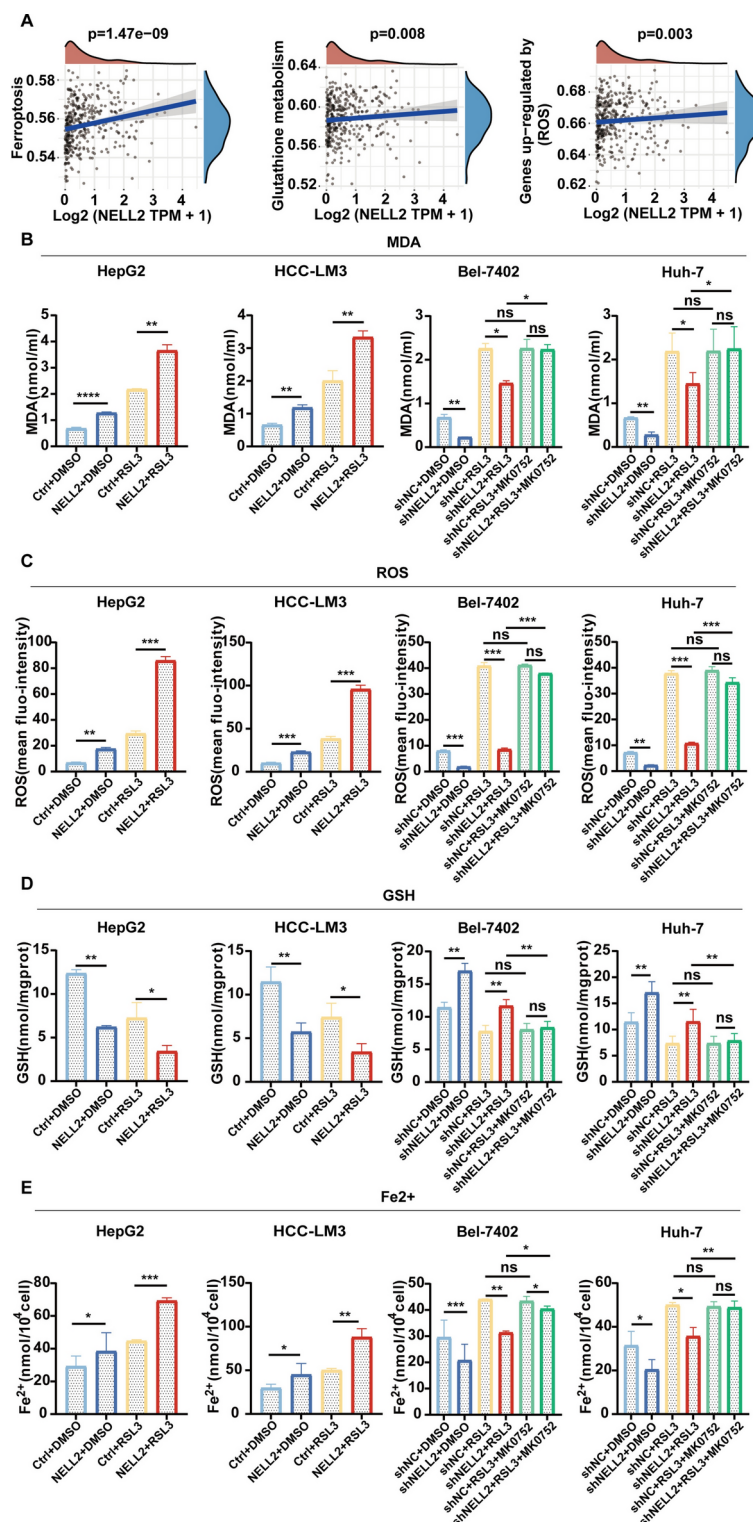


**Fig. 5.** (A) The relationship between the expression level of NELL2 and ferroptosis, glutathione metabolism, ROS using the data from TCGA; (B) The level of MDA in HCC cell lines after transfection with knockdown (Bel-7402, Huh-7) or overexpression (HepG2, HCC-LM3) lentiviruses treated with 5nM DMSO, 5nM RSL3 or 5nM RSL3 + 5nM MK0752 was detected; (C) The level of ROS in HCC cell lines after transfection with knockdown (Bel-7402, Huh-7) or overexpression (HepG2, HCC-LM3) lentiviruses treated with 5nM DMSO, 5nM RSL3 or 5nM RSL3 + 5nM MK0752 was detected; (D) The level of GSH in HCC cell lines after transfection with knockdown (Bel-7402, Huh-7) or overexpression (HepG2, HCC-LM3) lentiviruses treated with 5nM DMSO, 5nM RSL3 or 5nM RSL3 + 5nM MK0752 was detected, E. The level of Fe<sup>2+</sup> in HCC cell lines after transfection with knockdown (Bel-7402, Huh-7) or overexpression (HepG2, HCC-LM3) lentiviruses treated with 5nM DMSO, 5nM RSL3 or 5nM RSL3 + 5nM MK0752 was detected.



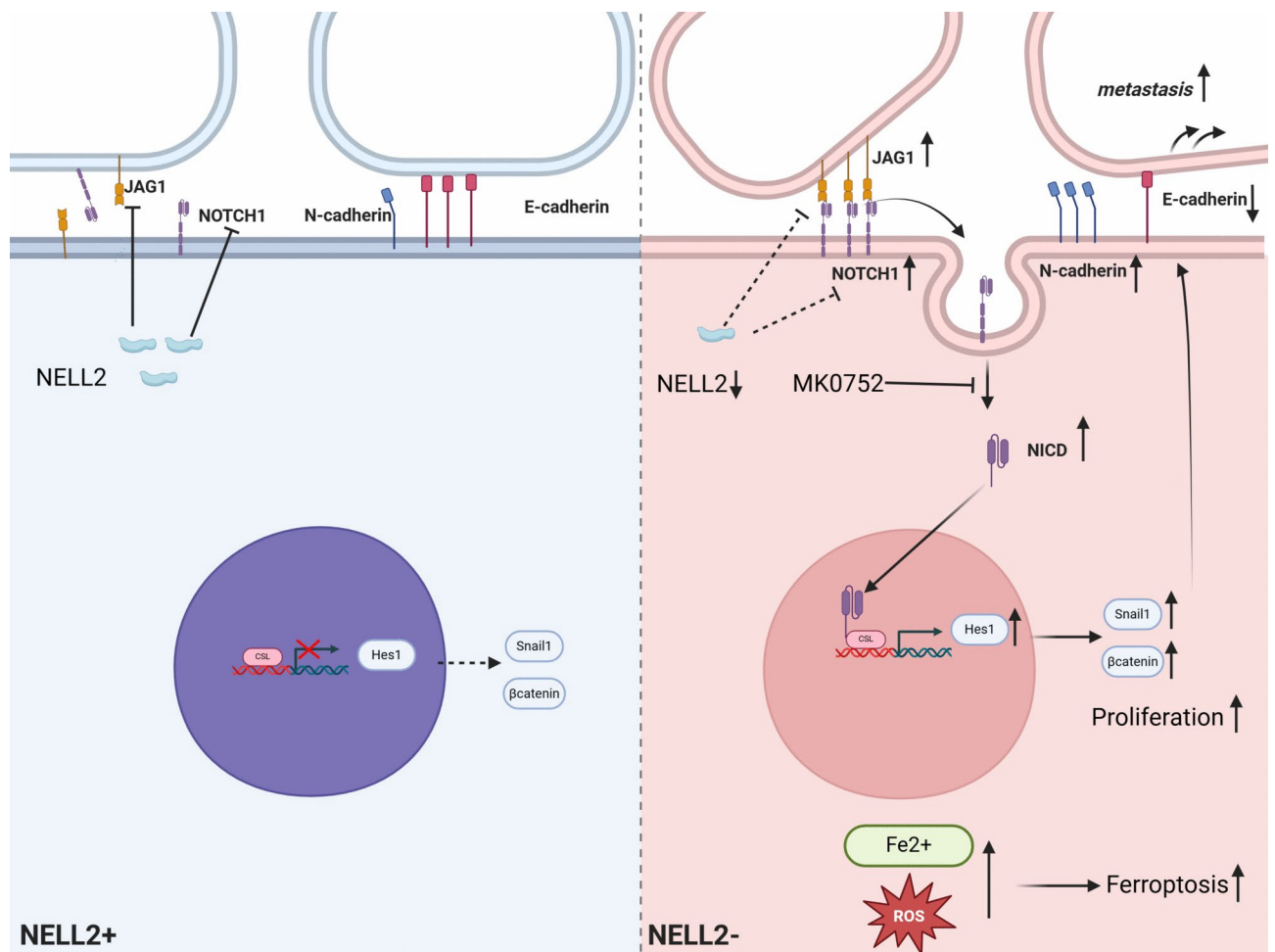


**Fig. 6.** Working model of NELL2 in hepatocellular carcinoma.

## Data availability

All data underlying this article are available in the article and in its online supplementary material. The data supporting this study's findings are available on request from the corresponding author.

Received: 26 April 2024; Accepted: 17 March 2025

Published online: 25 March 2025

## References

- Hepatocellular carcinoma. *Nat. Rev. Dis. Primers* **7**(1):7 (2021).
- Toh, M. R. et al. Global epidemiology and genetics of hepatocellular carcinoma. *Gastroenterology* **164**(5), 766–782 (2023).
- Bray, F. et al. Global cancer statistics 2022: GLOBOCAN estimates of incidence and mortality worldwide for 36 cancers in 185 countries. *CA Cancer J. Clin.* <https://doi.org/10.3322/caac.21834> (2024).
- Sia, D., Villanueva, A., Friedman, S. L. & Llovet, J. M. Liver cancer cell of origin, molecular class, and effects on patient prognosis. *Gastroenterology* **152**(4), 745–761 (2017).
- Peng, J., Lü, M., Peng, Y. & Tang, X. Global incidence of primary liver cancer by etiology among children, adolescents, and young adults. *J. Hepatol.* **79**(2), e92–e94 (2023).
- Goutté, N. et al. Geographical variations in incidence, management and survival of hepatocellular carcinoma in a Western country. *J. Hepatol.* **66**(3), 537–544 (2017).
- Zhu, H. D. et al. Transarterial chemoembolization with PD-(L)1 inhibitors plus molecular targeted therapies for hepatocellular carcinoma (CHANCE001). *Signal Transduct. Target Ther.* **8**(1), 58 (2023).
- Vitale, A. et al. Personalised management of patients with hepatocellular carcinoma: A multiparametric therapeutic hierarchy concept. *Lancet Oncol.* **24**(7), e312–e322 (2023).
- Jaworski, A. et al. Operational redundancy in axon guidance through the multifunctional receptor Robo3 and its ligand NELL2. *Science* **350**(6263), 961–965 (2015).
- Watanabe, T. K. et al. Cloning and characterization of two novel human cDNAs (NELL1 and NELL2) encoding proteins with six EGF-like repeats. *Genomics* **38**(3), 273–276 (1996).
- Ha, C. M. et al. NELL2, a neuron-specific EGF-like protein, is selectively expressed in glutamatergic neurons and contributes to the glutamatergic control of GnRH neurons at puberty. *Neuroendocrinology* **88**(3), 199–211 (2008).
- Jayabal, P. et al. NELL2-cdc42 signaling regulates BAF complexes and Ewing sarcoma cell growth. *Cell Rep.* **36**(1), 109254 (2021).
- Osman, I. et al. Novel blood biomarkers of human urinary bladder cancer. *Clin. Cancer Res.* **12**(11 Pt 1), 3374–3380 (2006).

14. Zhang, Z. et al. A novel basement membrane-related gene signature for prognosis of lung adenocarcinomas. *Comput. Biol. Med.* **154**, 106597 (2023).
15. Pak, J. S. et al. NELL2-Robo3 complex structure reveals mechanisms of receptor activation for axon guidance. *Nat. Commun.* **11**(1), 1489 (2020).
16. Kim, D. Y., Kim, H. R., Kim, K. K., Park, J. W. & Lee, B. J. NELL2 function in the protection of cells against endoplasmic reticulum stress. *Mol. Cells* **38**(2), 145–150 (2015).
17. Osborne, B. A. & Minter, L. M. Notch signalling during peripheral T-cell activation and differentiation. *Nat. Rev. Immunol.* **7**(1), 64–75 (2007).
18. Schneider, M., Allman, A. & Maillard, I. Regulation of immune cell development, differentiation and function by stromal Notch ligands. *Curr. Opin. Cell Biol.* **85**, 102256 (2023).
19. Espinoza, I. & Miele, L. Deadly crosstalk: Notch signaling at the intersection of EMT and cancer stem cells. *Cancer Lett.* **341**(1), 41–45 (2013).
20. Parida, S. et al. A procarcinogenic colon microbe promotes breast tumorigenesis and metastatic progression and concomitantly activates notch and  $\beta$ -catenin axes. *Cancer Discov.* **11**(5), 1138–1157 (2021).
21. Giovannini, C., Fornari, F., Piscaglia, F. & Gramantieri, L. Notch signaling regulation in HCC: From hepatitis virus to non-coding RNAs. *Cells* **10**(3), 521 (2021).
22. Greife, A., Hoffmann, M. J. & Schulz, W. A. Consequences of disrupted notch signaling in bladder cancer. *Eur. Urol.* **68**(1), 3–4 (2015).
23. Marignol, L., Rivera-Figueroa, K., Lynch, T. & Hollywood, D. Hypoxia, notch signalling, and prostate cancer. *Nat. Rev. Urol.* **10**(7), 405–413 (2013).
24. Nandagopal N, Santat LA, Elowitz MB: Cis-activation in the Notch signaling pathway. *Elife* **8**, (2019).
25. Kalafut, J. et al. Regulation of Notch1 signalling by long non-coding RNAs in cancers and other health disorders. *Int. J. Mol. Sci.* **24**(16), 12579 (2023).
26. Misiolek, J. O. et al. Context matters: NOTCH signatures and pathway in cancer progression and metastasis. *Cells* **10**(1), 94 (2021).
27. Grilli, G. et al. Impact of notch signaling on the prognosis of patients with head and neck squamous cell carcinoma. *Oral Oncol.* **110**, 105003 (2020).
28. Kunnimalaiyaan, M. & Chen, H. Tumor suppressor role of Notch-1 signaling in neuroendocrine tumors. *Oncologist* **12**(5), 535–542 (2007).
29. Ohmoto, A. et al. Clinicopathological and genomic features in patients with head and neck neuroendocrine carcinoma. *Mod. Pathol.* **34**(11), 1979–1989 (2021).
30. Xie, Y. et al. Ferroptosis: Process and function. *Cell Death Differ.* **23**(3), 369–379 (2016).
31. Ma, X. et al. Cholesterol induces CD8(+) T cell exhaustion in the tumor microenvironment. *Cell Metab.* **30**(1), 143–156.e145 (2019).
32. Mou, Y. et al. Ferroptosis, a new form of cell death: Opportunities and challenges in cancer. *J. Hematol. Oncol.* **12**(1), 34 (2019).
33. Wang, H. et al. The E3 ligase MIB1 promotes proteasomal degradation of NRF2 and sensitizes lung cancer cells to ferroptosis. *Mol. Cancer Res.* **20**(2), 253–264 (2022).
34. Li, R., Hu, Z., Qiao, Q., Zhou, D. & Sun, M. Anti-NOTCH1 therapy with OMP-52 M51 inhibits salivary adenoid cystic carcinoma by depressing epithelial-mesenchymal transition (EMT) process and inducing ferroptosis. *Toxicol. Appl. Pharmacol.* **484**, 116825 (2024).
35. Fassunke, J. et al. Array analysis of epilepsy-associated gangliogliomas reveals expression patterns related to aberrant development of neuronal precursors. *Brain* **131**(Pt 11), 3034–3050 (2008).
36. Wang, Y., Li, M., Zhang, L., Chen, Y. & Zhang, S. m6A demethylase FTO induces NELL2 expression by inhibiting E2F1 m6A modification leading to metastasis of non-small cell lung cancer. *Mol. Ther. Oncolytics* **21**, 367–376 (2021).
37. Alvarez-Díaz, S. et al. MicroRNA-22 is induced by vitamin D and contributes to its antiproliferative, antimigratory and gene regulatory effects in colon cancer cells. *Hum. Mol. Genet.* **21**(10), 2157–2165 (2012).
38. Bhosale, P. G. et al. Chromosomal alterations and gene expression changes associated with the progression of leukoplakia to advanced gingivobuccal cancer. *Transl. Oncol.* **10**(3), 396–409 (2017).
39. Liu, X. et al. Discovery of microarray-identified genes associated with ovarian cancer progression. *Int. J. Oncol.* **46**(6), 2467–2478 (2015).
40. Luo, J., Dunn, T. A., Ewing, C. M., Walsh, P. C. & Isaacs, W. B. Decreased gene expression of steroid 5 alpha-reductase 2 in human prostate cancer: Implications for finasteride therapy of prostate carcinoma. *Prostate* **57**(2), 134–139 (2003).
41. Nakamura, R. et al. Expression and regulatory effects on cancer cell behavior of NELL1 and NELL2 in human renal cell carcinoma. *Cancer Sci.* **106**(5), 656–664 (2015).
42. Liu, M. et al. A 15-gene signature and prognostic nomogram for predicting overall survival in non-distant metastatic oral tongue squamous cell carcinoma. *Front. Oncol.* **11**, 587548 (2021).
43. Li, Y. et al. Transcriptomics based multi-dimensional characterization and drug screen in esophageal squamous cell carcinoma. *EBioMedicine* **70**, 103510 (2021).
44. Tong, L. et al. The tRNA-derived fragment-3017A promotes metastasis by inhibiting NELL2 in human gastric cancer. *Front. Oncol.* **10**, 570916 (2020).
45. Nowell, C. S. & Radtke, F. Notch as a tumour suppressor. *Nat. Rev. Cancer* **17**(3), 145–159 (2017).
46. Huang, T. et al. NOTCH receptors in gastric and other gastrointestinal cancers: Oncogenes or tumor suppressors?. *Mol. Cancer* **15**(1), 80 (2016).
47. Hu, S. et al. NOTCH-YAP1/TEAD-DNMT1 axis drives hepatocyte reprogramming into intrahepatic cholangiocarcinoma. *Gastroenterology* **163**(2), 449–465 (2022).
48. Sharma, A. et al. Onco-fetal reprogramming of endothelial cells drives immunosuppressive macrophages in hepatocellular carcinoma. *Cell* **183**(2), 377–394.e321 (2020).
49. Yan, W. et al. Notch signaling regulates immunosuppressive tumor-associated macrophage function in pancreatic cancer. *Cancer Immunol. Res.* **12**(1), 91–106 (2024).
50. Lim, J. S. et al. Intratumoural heterogeneity generated by Notch signalling promotes small-cell lung cancer. *Nature* **545**(7654), 360–364 (2017).
51. Bocchicchio, S., Tesone, M. & Irusta, G. Convergence of Wnt and Notch signaling controls ovarian cancer cell survival. *J. Cell Physiol.* **234**(12), 22130–22143 (2019).
52. Diao, B., Sun, C., Yu, P., Zhao, Z. & Yang, P. LAMA5 promotes cell proliferation and migration in ovarian cancer by activating Notch signaling pathway. *Faseb J.* **37**(9), e23109 (2023).
53. Dandawate, P. et al. Cucurbitacin B and I inhibits colon cancer growth by targeting the Notch signaling pathway. *Sci. Rep.* **10**(1), 1290 (2020).
54. Deshmukh, A. P. et al. Identification of EMT signaling cross-talk and gene regulatory networks by single-cell RNA sequencing. *Proc. Natl. Acad. Sci. U. S. A.* <https://doi.org/10.1073/pnas.2102050118> (2021).
55. Yuan, X. et al. Notch signaling and EMT in non-small cell lung cancer: Biological significance and therapeutic application. *J. Hematol. Oncol.* **7**, 87 (2014).
56. Yang, X. et al. m(6) A-dependent modulation via IGF2BP3/MCM5/Notch axis promotes partial EMT and LUAD metastasis. *Adv. Sci. (Weinh.)* **10**(20), e2206744 (2023).

57. Jin, M. et al. MCUR1 facilitates epithelial-mesenchymal transition and metastasis via the mitochondrial calcium dependent ROS/Nrf2/Notch pathway in hepatocellular carcinoma. *J. Exp. Clin. Cancer Res.* **38**(1), 136 (2019).
58. Wang, Z. et al. Acquisition of epithelial-mesenchymal transition phenotype of gemcitabine-resistant pancreatic cancer cells is linked with activation of the notch signaling pathway. *Cancer Res.* **69**(6), 2400–2407 (2009).
59. Shaker, M. R. et al. Neural epidermal growth factor-like protein 2 is expressed in human oligodendroglial cell types. *Front. Cell Dev. Biol.* **10**, 803061 (2022).
60. Zhou, B. et al. Notch signaling pathway: Architecture, disease, and therapeutics. *Signal Transduct. Target. Ther.* **7**(1), 95 (2022).
61. Shi, Q. et al. Notch signaling pathway in cancer: From mechanistic insights to targeted therapies. *Signal Transduct. Target. Ther.* **9**(1), 128 (2024).
62. Cuervo, H., Mühleder, S., García-González, I. & Benedito, R. Notch-mediated cellular interactions between vascular cells. *Curr. Opin. Cell Biol.* **85**, 102254 (2023).
63. Zanolini, S. & Canalis, E. Notch signaling and the skeleton. *Endocrine Rev.* **37**(3), 223–253 (2016).
64. Jiang, X., Stockwell, B. R. & Conrad, M. Ferroptosis: Mechanisms, biology and role in disease. *Nat. Rev. Mol. Cell Biol.* **22**(4), 266–282 (2021).

## Author contributions

G.W, H.W and S.L conceived and designed this study. H.Z, D.W and P.Z obtained the data. H.W and S.L analyzed the data. H.W, S.L, Y.W, H.Y and R.X performed the experiments. P.Z, H.Y, R.X and Y.W prepared figures. G.W, H.W, H.Z, D.W and H.Y helped discuss the results. S.L. and H.W drafted the manuscript. G.W revised the manuscript. All authors contributed to the article and approved the submitted version.

## Funding

Central guidance for local scientific and technological development project (2024)JH6/100800030). Central guidance for local scientific and technological development project (2023)JH6/100100014).

## Declarations

## Competing interests

The authors declare no competing interests.

## Ethics approval and consent to participate

The experimental protocol was established according to the ethical guidelines of the Declaration of Helsinki and was approved by the Medicine Ethics Committee of the First Hospital of China Medical University (AF-SOP-07-1.1-01).

## Consent for publication

All the authors have read and agreed to the published version of the manuscript.

## Additional information

**Supplementary Information** The online version contains supplementary material available at <https://doi.org/10.1038/s41598-025-94669-9>.

**Correspondence** and requests for materials should be addressed to G.W.

**Reprints and permissions information** is available at [www.nature.com/reprints](http://www.nature.com/reprints).

**Publisher's note** Springer Nature remains neutral with regard to jurisdictional claims in published maps and institutional affiliations.

**Open Access** This article is licensed under a Creative Commons Attribution-NonCommercial-NoDerivatives 4.0 International License, which permits any non-commercial use, sharing, distribution and reproduction in any medium or format, as long as you give appropriate credit to the original author(s) and the source, provide a link to the Creative Commons licence, and indicate if you modified the licensed material. You do not have permission under this licence to share adapted material derived from this article or parts of it. The images or other third party material in this article are included in the article's Creative Commons licence, unless indicated otherwise in a credit line to the material. If material is not included in the article's Creative Commons licence and your intended use is not permitted by statutory regulation or exceeds the permitted use, you will need to obtain permission directly from the copyright holder. To view a copy of this licence, visit <http://creativecommons.org/licenses/by-nc-nd/4.0/>.

© The Author(s) 2025